nature neuroscience

SUPPLEMENTARY INFORMATION

https://doi.org/10.1038/s41593-020-0630-x

In the format provided by the authors and unedited.

Within-group synchronization in the prefrontal cortex associates with intergroup conflict

Jiaxin Yang[1], Hejing Zhang[1], Jun Ni[1], Carsten K. W. De Dreu[2,3] and Yina Ma[1]✉

[1]State Key Laboratory of Cognitive Neuroscience and Learning, IDG/McGovern Institute for Brain Research, Beijing Key Laboratory of Brain Imaging and Connectomics, Beijing Normal University, Beijing, China. [2]Institute of Psychology, Leiden University, Leiden, The Netherlands. [3]Center for Research in Experimental Economics and Political Decision Making, University of Amsterdam, Amsterdam, The Netherlands. ✉e-mail: yma@bnu.edu.cn

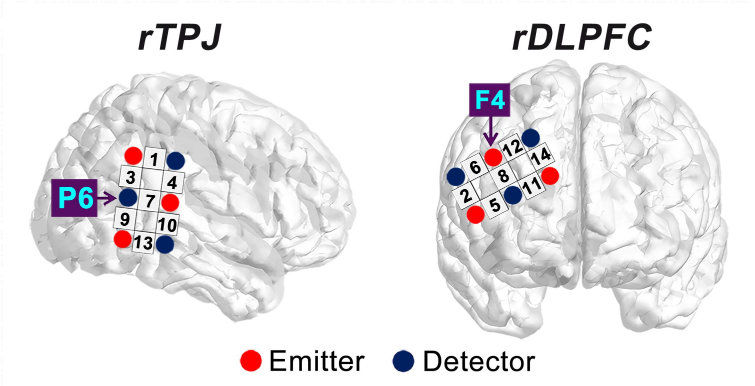

Supplementary Figure 1 | Illustration of fNIRS Optode Position.

We used two identical 3 × 2 optode probe sets, with each probe set (inter-optode distance of 30 mm) consisting of 3 light emitters (red) and 3 detectors (blue), and 7 channels. Each probe set was separately placed on the right temporo-parietal junction (rTPJ) or the right dorsolateral prefrontal cortex (rDLPFC) according to the relevant standard positions of P6 and F4 in the international 10-10 system for electroencephalogram electrode placement[1-4].

References:

1. Koessler, L. et al. Automated cortical projection of EEG sensors: anatomical correlation via the international 10–10 system. *Neuroimage* **46**, 64-72 (2009).
2. Luck, S. J. An introduction to the event-related potential technique (MIT press, 2014).
3. Tang, H. et al. Interpersonal brain synchronization in the right temporo-parietal junction during face-to-face economic exchange. *Soc. Cogn. Affect. Neurosci.* **11**, 23-32 (2015).
4. Lu, K., Xue, H., Nozawa, T. & Hao, N. Cooperation makes a group be more creative. *Cereb. Cortex* **22**, 1-14 (2018).

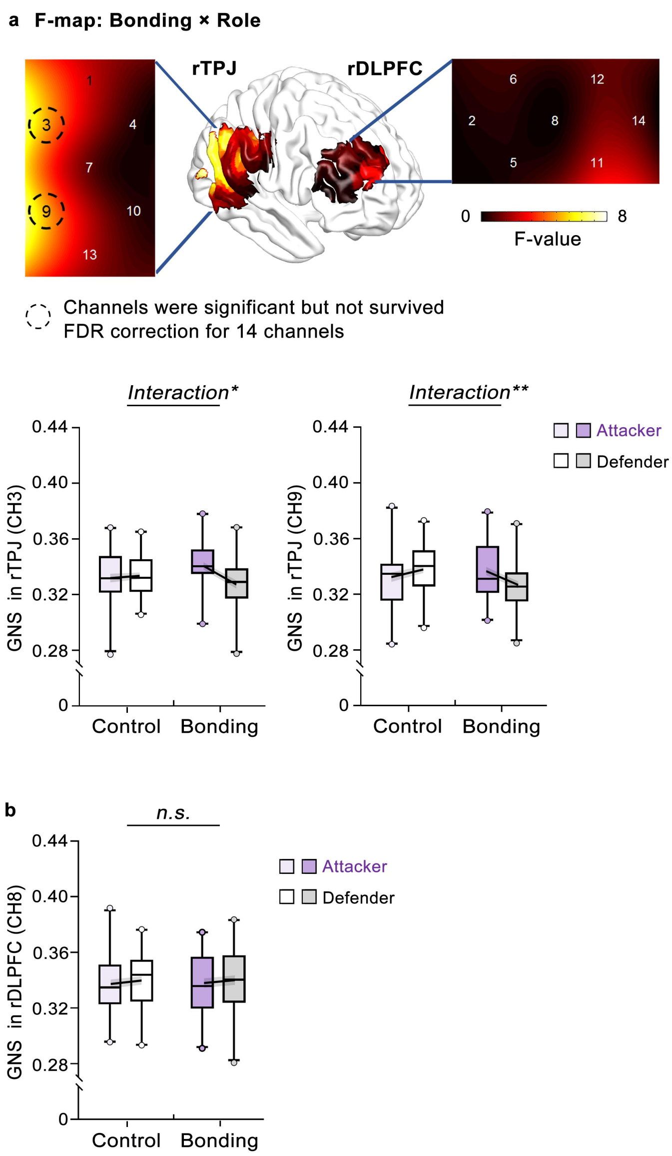

Supplementary Figure 2 | GNS and group-averaged activity based on the deoxygenated hemoglobin (Deoxy-Hb) signal.

We similarly applied the wavelet-based global noise removal technique to Deoxy-Hb time series and performed Wavelet Transform Coherence analysis to calculate the GNS of Deoxy-Hb signal for each three-person group. **a,** The F-map of the Bonding × Role interaction on GNS. We found a similar Bonding × Role interaction effect at channels 3 and 9 of rTPJ (channel 3: $F_{1,84} = 6.777$, $p = 0.011$, $\eta^2 = 0.075$; channel 9: $F_{1,84} = 6.999$, $p = 9.73\times10^{-3}$, $\eta^2 = 0.077$) but did not survive from FDR-correction for 14 channels. **b,** Regarding the GNS for channels 8, 11, 4, and 13, although the pattern at channel 8 was similar to that observed in Oxy-Hb analysis, there were no significant Bonding × Role interaction ($F_{1,84} = 0.006$, $p = 0.938$, $\eta^2 = 7.14 \times 10^{-5}$). Mixed-model ANOVAs, $n = 86$ three-versus-three-person intergroup contest sessions. Data are plotted as boxplots for each condition in which horizontal lines indicate median values, boxes indicate 25/75% quartiles, and whiskers indicate the 2.5-97.5% percentile range. Data points outside the range are shown separately as circles. Solid lines start from the mean and reflect the intervals for the Mean ± S.E. * $p < 0.05$, ** $p < 0.01$. *n.s.* not significant.

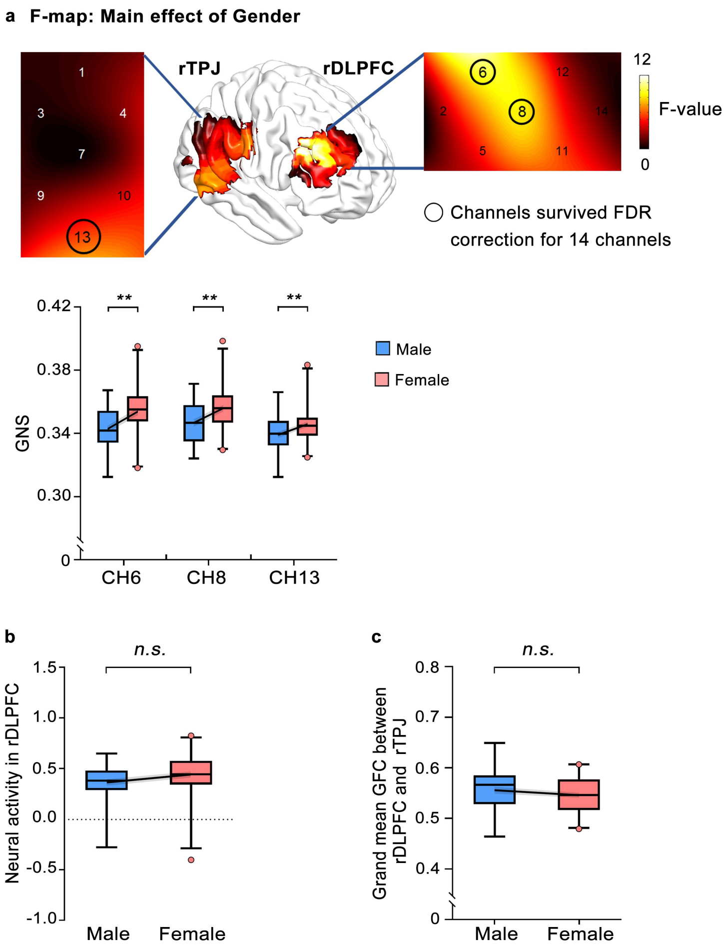

Supplementary Figure 3 | Gender Effect.

All sessions were classified as all-male sessions ($n = 38$ six-person sessions) and all-female sessions ($n = 48$ six-person sessions). To examine whether session gender influenced the neural response (including GNS, within-group averaged neural activity and group-averaged functional connectivity), we included Session gender (all-male *vs.* all-female sessions) as a between-session factor. **a,** Session gender produced a main effect showing stronger GNS in the rDLPFC (*ps* < 0.05, FDR correction, channel 6: $F_{1,82} = 11.085$, $p = 1.31\times10^{-3}$, $\eta^2 = 0.119$; channel 8: $F_{1,82} = 8.698$, $p = 0.004$, $\eta^2 = 0.096$) and rTPJ (channel 13: $F_{1,82} = 7.142$, $p = 0.009$, $\eta^2 = 0.080$) in all-female sessions than all-male sessions, but Session gender did not interact with Bonding or Role (*ps* > 0.05, Supplementary Table 10a provides the full statistical report of each channel). **b, c,** There was no effect of Session gender on within-group averaged neural activity **(**$F_{1,82} = 2.815$, $p = 0.097$, $\eta^2 = 0.033$) nor group-averaged functional connectivity ($F_{1,82} = 1.169$, $p = 0.283$, $\eta^2 = 0.014$, Supplementary Table 10c provides the full statistical report of each channel pair). Mixed-model ANOVAs on 86 three-versus-three-person intergroup contest sessions. Data are plotted as boxplots for each condition in which horizontal lines indicate median values, boxes indicate 25/75% quartiles, and whiskers indicate the 2.5-97.5% percentile range. Data points outside the range are shown separately as circles. Solid lines start from the mean and reflect the intervals for the Mean ± S.E. ** $p < 0.01$, *n.s.* not significant.

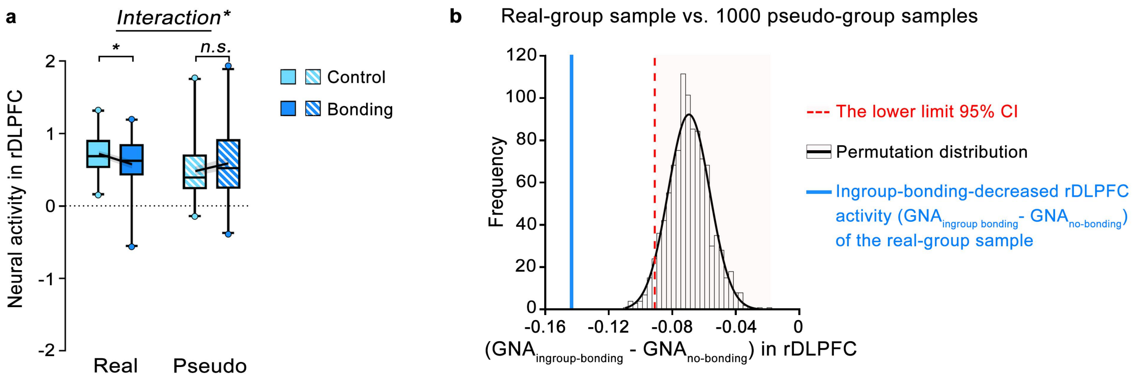

Supplementary Figure 4 | Stronger Bonding effect on group-level rDLPFC activity in real than pseudo groups.

a, We conducted Role (attacker vs. defender) × Bonding (in-group bonding vs. no-bonding control) × Group (real vs. pseudo groups) ANOVA on the group-level neural activity (GNA) in rDLPFC (i.e. channel 8), 86 six-person real groups and 86 six-person pseudo groups. We found significant interactions of Bonding and Group when comparing real groups with pseudo groups ($F_{1,168} = 4.053$, $p = 0.046$, $\eta^2 = 0.024$). The reduced rDLPFC activity following in-group bonding (vs. non-bonding control) was only observed in the real group ($F_{1,84} = 4.034$, $p = 0.048$, $\eta^2 = 0.046$), but not the pseudo group ($F_{1,84} = 1.108$, $p = 0.296$, $\eta^2 = 0.013$). Mixed-model ANOVAs, 86 six-person groups, respectively for real and pseudo groups. Data are plotted as boxplots for each condition in which horizontal lines indicate median values, boxes indicate 25/75% quartiles, and whiskers indicate the 2.5-97.5% percentile range. Data points outside the range are shown separately as circles. Solid lines start from the mean and reflect the intervals for the Mean ± S.E. * $p < 0.05$, *n.s.* not significant. **b,** One-sided permutation test was used to verify the stronger Bonding effect on group-level rDLPFC activity in real than pseudo groups. We compared the real-group sample with 1000 pseudo-group samples[1-4]. We tested the ingroup-bonding-decreased group-level nerual activity in the rDLPFC ($GNA_{ingroup\text{-}bonding} - GNA_{no\text{-}bonding}$) of the real-group sample against permutation samples based on the mean differences of rDLPFC activity between in-group bonding and no-bonding control ($n = 1000$, each permutation sample contains 172 within-condition three-person pseudo groups). We showed that the observed ingroup-bonding-decreased group-level rDLPFC activity in the real groups was outside the lower limit of 95% *CI* of the permutation distribution.

References:

1. Jiang, J. et al. Leader emergence through interpersonal neural synchronization. *Proc. Natl. Acad. Sci. U.S.A.* **112**, 4274-4279 (2015).
2. Dai, B. et al. Neural mechanisms for selectively tuning into the target speaker in a naturalistic noisy situation. *Nature Comm.* **9**, 2405-2416 (2018).
3. Bilek, E. et al. Information flow between interacting human brains: Identification, validation, and relationship to social expertise. *Proc. Natl. Acad. Sci. U.S.A.* **112**, 5207-5212 (2015).
4. Bilek, E. et al. State-dependent cross-brain information flow in borderline personality disorder. *JAMA psychiatry* **74**, 949-957 (2017).

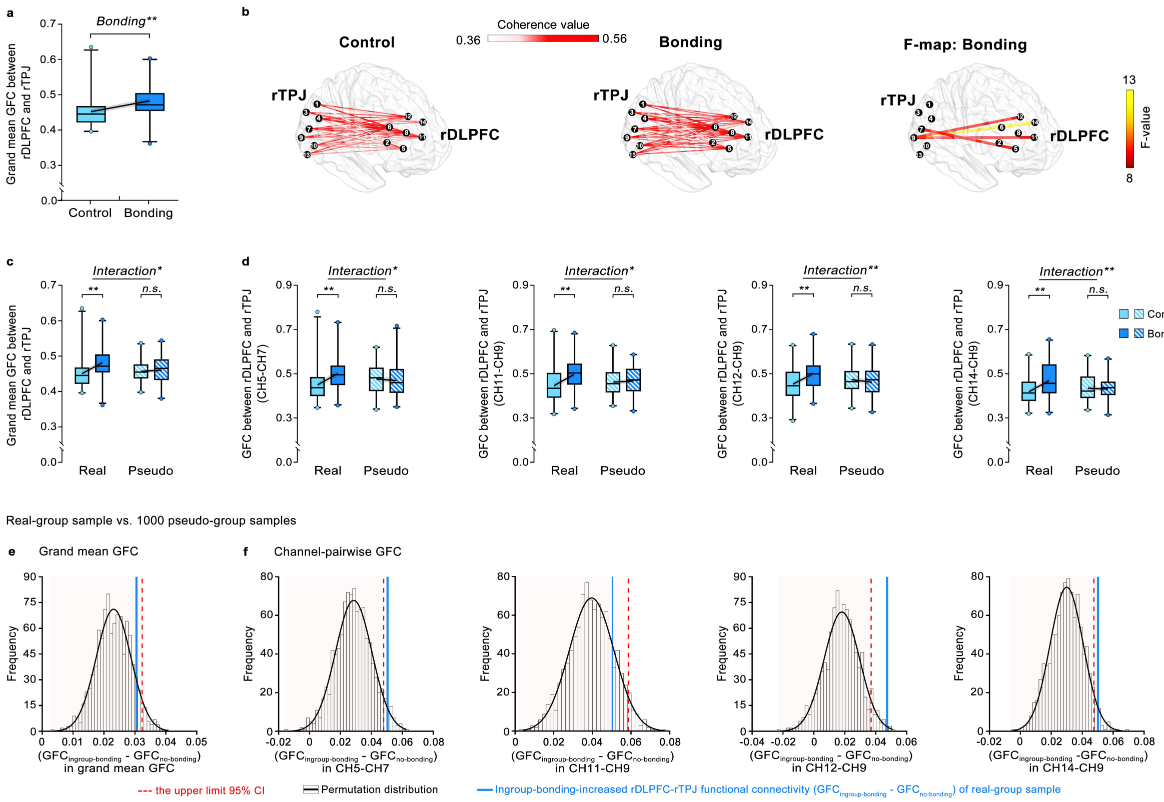

Supplementary Figure 5 | Stronger Bonding effect on group-level rDLPFC-rTPJ connectivity in real than pseudo groups.

a, b, We conducted Bonding (in-group bonding vs. no-bonding control) × Role (attacker vs. defender) ANOVAs (n = 86 three-versus-three-person intergroup contest sessions) on the grand-mean rDLPFC-rTPJ functional connectivity (**a**) and channel-pairwise rDLPFC-rTPJ functional connectivity in the real groups (**b**). We found that the increased group-level functional connectivity (GFC) following in-group bonding (vs. non-bonding control) in both grand mean rDLPFC-rTPJ connectivity (**a,** $F_{1,84}$ = 9.047, p = 0.003, η^2 = 0.097), and channel-pairwise rDLPFC–rTPJ connectivity (**b,** CH5-CH7: $F_{1,84}$ = 9.126, p = 0.003, η^2 = 0.098; CH11-CH9: $F_{1,84}$ = 8.952, p = 0.004, η^2 = 0.096; CH12-CH9: $F_{1,84}$ = 8.783, p = 0.004, η^2 = 0.095; CH14-CH9: $F_{1,84}$ = 11.320, p = 1.16×10^{-3}, η^2 = 0.119; survived from FDR correction for 49 channel-pairs). **c, d,** We conducted Bonding (in-group bonding vs. no-bonding control) × Role (attacker vs. defender) × Group (real vs. pseudo groups) ANOVAs on the group-level rDLPFC-rTPJ functional connectivity (86 six-person real groups and 86 six-person pseudo groups). We found significant interactions of Bonding and Group when comparing real groups with pseudo groups (**c,** grand mean level: $F_{1,168}$ = 4.406, p = 0.037, η^2 = 0.026; **d,** channel-pairwise level: CH5-CH7: $F_{1,168}$ = 5.871, p = 0.016, η^2 = 0.034; CH11-CH9: $F_{1,168}$ = 4.429, p = 0.037, η^2 = 0.026; CH12-CH9: $F_{1,168}$ = 6.892, p = 0.009, η^2 = 0.039; CH14-CH9: $F_{1,168}$ = 7.398, p = 0.007, η^2 = 0.042; survived FDR correction for the 4 testing channel-pairs). The increased rDLPFC-rTPJ functional connectivity following in-group bonding (vs. non-bonding control) was only observed in real groups (**a-d**), but not pseudo groups (**c,** grand mean level: $F_{1,84}$ = 0.224, p = 0.638, η^2 = 0.003; **d,**

channel-pairwise level: CH5-CH7: $F_{1,84} = 0.169$, $p = 0.682$, $\eta^2 = 0.002$; CH11-CH9: $F_{1,84} = 0.094$, $p = 0.759$, $\eta^2 = 0.001$; CH12-CH9: $F_{1,84} = 0.534$, $p = 0.467$, $\eta^2 = 0.006$; CH14-CH9: $F_{1,84} = 0.088$, $p = 0.767$, $\eta^2 = 0.001$). Mixed-model ANOVAs, 86 three-versus-three-person intergroup contest sessions for pseudo groups. Data are plotted as boxplots for each condition in which horizontal lines indicate median values, boxes indicate 25/75% quartiles, and whiskers indicate the 2.5–97.5% percentile range. Data points outside the range are shown separately as circles. Solid lines start from the mean and reflect the intervals of Mean ± S.E. * $p < 0.05$, ** $p < 0.01$. **e, f,** We compared the Bonding effect on rDLPFC-rTPJ connectivity between real and pseudo groups using one-sided permutation test. Specifically, for both grand mean GFC and channel-pairwise GFC, we compared the real-group sample with 1000 pseudo-group samples[1-4]. We tested the ingroup-bonding-increased rDLPFC-rTPJ functional connectivity ($GFC_{ingroup\text{-}bonding} - GFC_{no\text{-}bonding}$) of the real-group sample against permutation samples based on the mean differences of GFC between in-group bonding and no-bonding control in pseudo-group samples ($n = 1000$, each permutation sample contains 172 within-condition three-person pseudo groups). We showed that the observed ingroup-bonding-increased rDLPFC-rTPJ connectivity in real groups were outside the upper limit of 95% CI of the permutation distribution (at channel-pairs: CH5 - CH7; CH12 - CH9: $p = 0.005$; and CH14 - CH9).

References:

1. Jiang, J. et al. Leader emergence through interpersonal neural synchronization. *Proc. Natl. Acad. Sci. U.S.A.* **112**, 4274-4279 (2015).
2. Dai, B. et al. Neural mechanisms for selectively tuning into the target speaker in a naturalistic noisy situation. *Nature Comm.* **9**, 2405-2416 (2018).
3. Bilek, E. et al. Information flow between interacting human brains: Identification, validation, and relationship to social expertise. *Proc. Natl. Acad. Sci. U.S.A.* **112**, 5207-5212 (2015).
4. Bilek, E. et al. State-dependent cross-brain information flow in borderline personality disorder. *JAMA psychiatry* **74**, 949-957 (2017).

Supplementary Table 1 | Matched demographic and psychological information among four conditions.

a, Behavioral data analysis sample (*n* = 91 intergroup contest sessions)

Measurement	No-bonding control		Ingroup-bonding		Bonding	Role	Interaction
	Attacker	Defender	Attacker	Defender			
	Mean (SE)	Mean (SE)	Mean (SE)	Mean (SE)	*p*	*p*	*p*
● **Demographic information**							
Number of sessions (*n*)	44	44	47	47	-	-	-
Session gender (n_{male} vs. n_{female})	18 *vs.* 26	18 *vs.* 26	22 *vs.* 25	22 *vs.* 25	-	-	-
Age (year)	21.94 (0.26)	21.07 (0.21)	22.04 (0.25)	22.47 (0.24)	0.12	0.64	0.11
Education year	16.67 (0.18)	16.67 (0.12)	16.77 (0.16)	17.16 (0.17)	0.08	0.20	0.22
● **Psychological information**							
Empathic capacity	2.40 (0.03)	2.33 (0.03)	2.35 (0.03)	2.39 (0.03)	0.89	0.75	0.08
Cooperative personality	3.77 (0.04)	3.82 (0.03)	3.84 (0.05)	3.86 (0.05)	0.17	0.46	0.66
Social value orientation	25.11 (1.08)	26.18 (1.22)	25.55 (1.10)	26.88 (1.19)	0.60	0.33	0.92
Prosocial personality	3.18 (0.03)	3.16 (0.04)	3.17 (0.04)	3.21 (0.04)	0.70	0.84	0.33
Impulsiveness	3.12 (0.03)	3.12 (0.03)	3.13 (0.03)	3.10 (0.03)	0.84	0.56	0.63
Justice sensitivity	2.78 (0.07)	2.78 (0.05)	2.70 (0.06)	2.75 (0.05)	0.41	0.64	0.69
Preference for social hierarchy	3.30 (0.06)	3.40 (0.07)	3.43 (0.07)	3.32 (0.07)	0.67	0.97	0.09
Intergroup discrimination (iDG0)	6.02 (0.58)	6.60 (0.60)	7.28 (0.74)	7.23 (0.58)	0.14	0.67	0.62

b, *f*NIRS analysis sample (*n* = 86 sessions)

Measurement	No-bonding control		Ingroup-bonding		Bonding	Role	Interaction
	Attacker	Defender	Attacker	Defender			
	Mean (SE)	Mean (SE)	Mean (SE)	Mean (SE)	*p*	*p*	*p*
● **Demographic information**							
Number of sessions (*n*)	43	43	43	43	-	-	-
Session gender (n_{male} vs. n_{female})	18 *vs.* 25	18 *vs.* 25	20 *vs.* 23	20 *vs.* 23	-	-	-
Age (year)	21.86 (0.25)	21.70 (0.21)	22.03 (0.26)	22.46 (0.26)	0.09	0.54	0.17
Education year	16.61 (0.18)	16.67 (0.12)	16.77 (0.17)	17.12 (0.18)	0.07	0.19	0.34
● **Psychological information**							
Empathic capacity	2.40 (0.03)	2.33 (0.03)	2.34 (0.03)	2.39 (0.03)	0.97	0.61	0.06
Cooperative personality	3.77 (0.04)	3.82 (0.03)	3.84 (0.05)	3.87 (0.05)	0.18	0.40	0.76
Social value orientation	25.11 (1.10)	26.34 (1.23)	25.46 (1.18)	26.56 (1.27)	0.80	0.36	0.96
Prosocial personality	3.19 (0.04)	3.16 (0.04)	3.13 (0.04)	3.20 (0.04)	0.86	0.49	0.18
Impulsiveness	3.12 (0.03)	3.12 (0.03)	3.13 (0.03)	3.09 (0.03)	0.67	0.57	0.44
Justice sensitivity	2.78 (0.07)	2.78 (0.05)	2.71 (0.06)	2.77 (0.05)	0.49	0.62	0.61
Preference for social hierarchy	3.31 (0.06)	3.39 (0.07)	3.47 (0.07)	3.32 (0.07)	0.55	0.62	0.09
Intergroup discrimination (iDG0)	6.07 (0.59)	6.55 (0.61)	7.26 (0.79)	7.05 (0.61)	0.20	0.83	0.60

Note: We conducted 2 (Bonding: in-group bonding vs. no-bonding control) × 2 (Role: attacker vs. defender) mixed-model ANOVAs (n = 91 three-versus-three-person intergroup contest sessions for **a** and n = 86 three-versus-three-person contest sessions for **b**) on the demographic information and social-related traits. Empathic capacity was measured using the Interpersonal Reactivity Index[1], which consists of 28 items on a 5-point (0-4) Likert scale (higher scores reflecting more empathic of an individual). Cooperative personality was measured by the cooperative subscale of the Cooperation and Competition Personality scale[2] (13 items on a 5-point (1-5) Likert scale). Social value orientation was measured by the 6 primary items of the Social Value Orientation Slider task[3]. Prosocial personality was measured by the Social Responsibility, Other-Oriented Moral Reasoning, and Mutual Concerns Moral Reasoning subscales of Prosocial Personality Battery[4], which consists of 13 items on a 5-point (1-5) Likert scale (higher values reflecting more prosocial of an individual). Impulsiveness was measured using BAS subscale of the Behavioral Inhibition/Behavioral Activation Scales, BIS/BAS[5], which consists of 13 items on 4-point (1-4) Likert scale (higher values reflecting more appetitive motives). Justice sensitivity was measured using Justice Sensitivity Inventory[6], which consists of 40 items on 6-point (0-5) Likert scale (higher values reflecting more sensitive to justice). Individual's preference for social hierarchy was measured using Social Dominance Orientation (SDO) scale[7], which consists of 16 items on 7-point (1-7) Likert scale (higher values reflecting stronger preference for inequality among social groups). The individual's baseline intergroup discrimination was indexed by the intergroup bias in the intergroup Dictator Game (iDG0: split 20 monetary units between in-group and out-group members).

References:

1. Davis, M. H. Measuring individual differences in empathy: Evidence for a multidimensional approach. *J. Pers. Soc. Psychol*. **44**, 113-126 (1983).
2. Xie, X., Yu, Y., Chen, X. & Chen, X. P. The Measurement of Cooperative and Competitive Personality. *Acta. Psychologica. Sinica.* **38**, 116-125 (2006).
3. Murphy, R. O., Ackermann, K. A. & Handgraaf, M. Measuring social value orientation. *Judgm. Decis. Mak*. **6**, 771-781 (2011).
4. Penner, L. A. Dispositional and organizational influences on sustained volunteerism: An interactionist perspective. *J. Soc. Issues* **58**, 447-467 (2002).
5. Carver, C. S. & White, T. L. Behavioral inhibition, behavioral activation, and affective responses to impending reward and punishment: the BIS/BAS scales. *J. Pers. Soc. Psychol*. **67**, 319-333 (1994).
6. Schmitt, M., Baumert, A., Gollwitzer, M. & Maes, J. The justice sensitivity inventory: Factorial validity, location in the personality facet space, demographic pattern, and normative data. *Soc. Justice Res*. **23**, 211-238 (2010).
7. Sidanius, J., Levin, S., Liu, J. & Pratto, F. Social dominance orientation, anti-egalitarianism and the political psychology of gender: an extension and cross-cultural replication. *Eur. J. Soc. Psychol*. **30**, 41-67 (2000).

Supplementary Table 2 | Payoff matrix of one-round intergroup contest game.

Group	Role	Initial endowment (MU)	Individual contribution (x_i / y_i)	Group's pool C ($0 \le C \le 60$)	Payoff: Attackers lose $C_A \le C_D$	Payoff: Attackers win $C_A > C_D$
Attacker group	Attacker$_1$	20	x_1	$C_A = (x_1 + x_2 + x_3)$	$20 - x_1$	$20 - x_1 + (60 - C_D)/3$
	Attacker$_2$	20	x_2		$20 - x_2$	$20 - x_2 + (60 - C_D)/3$
	Attacker$_3$	20	x_3		$20 - x_3$	$20 - x_3 + (60 - C_D)/3$
Defender group	Defender$_1$	20	y_1	$C_D = (y_1 + y_2 + y_3)$	$20 - y_1$	0
	Defender$_2$	20	y_2		$20 - y_2$	0
	Defender$_3$	20	y_3		$20 - y_3$	0

Note: For each intergroup contest round, each individual received an initial endowment of 20 Monetary Units (MUs). Members of attacker (defender) group could each contribute x (y) out of 20 MUs. Each individual decided the amount (x_i for attacker group, and y_i for defender group, $0 \le x_i \le 20$, $0 \le y_i \le 20$) to the group's pool C ($0 \le C \le 60$, $C_A = [x_1 + x_2 + x_3]$, $C_D = [y_1 + y_2 + y_3]$). When $C_A \le C_D$, defender group would survive attacker group's attack and the members of both groups would earn what remained from their endowment (i.e., $20 - \{x, y\}$). When $C_A > C_D$, defender group failed and left with 0. Attacker group won and took away defender group's remaining MU ($60 - C_D$), which were divided equally among members of attacker group (each member: $[(60 - C_D)/3]$) and added to their remaining endowments ($20 - x_i$).

Supplementary Table 3 | Full statistical reports for behavioral indices in the intergroup contest game.

a, Descriptive statistics in each condition (*n* = 91 intergroup contest sessions)

Behavioral indices		No-bonding control (*n* = 44)		Ingroup-bonding (*n* = 47)	
		Attacker	Defender	Attacker	Defender
Contribution	Mean ± SE	5.77 ± 0.47	8.50 ± 0.41	6.90 ± 0.63	10.13 ± 0.43
	95% *CI*	4.83 - 6.71	7.68 - 9.32	5.63 - 8.17	9.26 - 11.00
Within-group decision coordination	Mean ± SE	0.19 ± 0.04	0.55 ± 0.05	0.34 ± 0.04	0.64 ± 0.05
	95% *CI*	0.11 - 0.27	0.45 - 0.65	0.25 - 0.43	0.53 - 0.75
Intergroup discrimination (iDG)	Mean ± SE	4.82 ± 0.69	8.41 ± 0.77	9.81 ± 0.61	11.23 ± 0.66
	95% *CI*	3.43 - 6.20	6.85 - 9.97	8.58 - 11.04	9.90 - 12.55
Intergroup discrimination (Likability)	Mean ± SE	0.52 ± 0.23	1.62 ± 0.23	1.55 ± 0.18	2.00 ± 0.22
	95% *CI*	0.07 - 0.98	1.16 - 2.08	1.18 - 1.92	1.56 - 2.44

b, Results of Bonding × Role mixed-model ANOVAs (*n* = 91 sessions)

Behavioral indices	Effect	*F*	*p*	η^2
Contribution	**Bonding**	4.133	**0.045***	0.044
	Role	279.194	**3.48×10^{-29}*** **	0.758
	Bonding × Role	1.937	0.167	0.021
Within-group decision coordination	**Bonding**	4.517	**0.036***	0.048
	Role	81.249	**3.52×10^{-14}*** **	0.477
	Bonding × Role	0.510	0.477	0.006
Intergroup discrimination	**Bonding**	32.786	**1.37×10^{-7}*** **	0.269
	Role	13.469	**4.13×10^{-4}*** **	0.131

(iDG)	Bonding × Role	2.530	0.115	0.028
Intergroup discrimination (Likability)	**Bonding**	12.625	**6.11×10^{-4}*** **	0.124
	Role	11.386	**1.10×10^{-3}** **	0.113
	Bonding × Role	2.025	0.158	0.022

Note: Contribution was calculated by the averaging contributions within 3-person group and across 24 rounds (range: 0-20 monetary units). Within-group decision coordination was calculated by correlating the 24-round contributions of each pair of two participants within each 3-person group (resulting in 3 correlations per group) and averaging the 3 Fisher z-transformed correlation coefficients. Higher value indicates higher coordination in round-level contributions among the group members. The intergroup discrimination in the intergroup Dictator Game (iDG) was calculated by subtracting donations to out-group members from those to in-group members. Higher value indicates stronger intergroup discrimination. The intergroup discrimination in the likability rating was calculated by subtracting likability rating of out-group members from those to in-group members. Higher value indicates stronger intergroup discrimination. Mixed-model ANOVAs, *n* = 91 three-versus-three-person intergroup contest sessions. Effects and p-values in bold indicate significant effects, * $p < 0.05$, ** $p < 0.01$, *** $p < 0.001$.

Supplementary Table 4 | The anatomical position for each channel.

Channel	MNI coordinates				BA	Brain Regions
	x	*y*	*z*	*SD*		
rDLPFC						
2	55	38	18	7.51	BA45	Inferior Frontal Gyrus
5	47	54	12	7.40	BA46	Dorsolateral prefrontal cortex
6	49	37	34	7.41	BA45	Middle Frontal Gyrus
8	40	53	28	6.81	BA46	Dorsolateral Prefrontal Cortex
11	27	65	22	6.78	BA10	Dorsolateral Prefrontal Cortex
12	29	48	43	6.77	BA9	Dorsolateral Prefrontal Cortex
14	18	60	36	6.23	BA9	Dorsolateral Prefrontal Cortex
rTPJ						
1	59	-51	48	11.40	BA40	Inferior Parietal Lobe
3	55	-68	35	11.95	BA39	Temporal Parietal Junction
4	67	-43	35	11.38	BA40	Supramarginal gyrus
7	64	-58	20	11.96	BA22	Superior Temporal Gyrus
9	57	-73	6	12.18	BA37	Middle Temporal Gyrus
10	69	-48	4	11.51	BA22	Middle Temporal Gyrus
13	62	-62	-10	13.65	BA37	Inferior Temporal Gyrus

Note: To further confirm the anatomical position of the optode probe sets, the high-resolution T1-weighted structural images from 6 participants (4 males, Mean ± SD = 22.5 ± 2.26 years) were acquired using a 3-T Siemens Trio scanner at the MRI Research Centre, Beijing Normal University. For each participant, we normalized the structural image in SPM8 and then obtained the MNI coordinates of 14 channels through NIRS-SPM toolbox. Across participants, we calculated the mean MNI coordinates and standard deviation for each channel[1]. The anatomical coordinates of each optode were shown in the Table and further confirmed the anatomical localization of right rTPJ and rDLPFC.

References:

1. Okamoto. M. et al. Three-dimensional probabilistic anatomical cranio-cerebral correlation via the international 10–20 system oriented for transcranial functional brain mapping. *Neuroimage* **21**, 99-111 (2004).

Supplementary Table 5 | Full statistical reports of the within-group neural synchronization (GNS).

a, Results of Bonding × Role interaction on GNS (*n* = 86 sessions intergroup contest sessions)

Channel	*F*	*p*	η^2	FDR- corrected *p*
rDLPFC				
2	0.005	0.942	6.34×10^{-5}	0.942
5	0.613	0.436	0.007	0.610
6	0.067	0.796	0.001	0.857
8	10.762	0.002**	0.114	**0.011***
11	8.868	0.004**	0.095	**0.018***
12	0.225	0.637	0.003	0.810
14	4.843	0.031*	0.055	0.071
rTPJ				
1	0.675	0.414	0.008	0.610
3	5.132	0.026*	0.058	0.071
4	6.837	0.011*	0.075	**0.037***
7	3.358	0.070	0.038	0.141
9	2.347	0.129	0.027	0.226
10	0.130	0.719	0.002	0.839
13	11.579	1.02×10^{-3}**	0.121	**0.011***

b, Descriptive statistics for the GNS in each condition for the survived channels (*n* = 86 sessions)

Channel	Indices	No-bonding control (*n* = 43)		In-group bonding (*n* = 43)	
		Attacker	Defender	Attacker	Defender
rDLPFC					
8	Mean ± SE	0.346 ± 0.003	0.359 ± 0.003	0.355 ± 0.003	0.348 ± 0.003
	95% *CI*	0.340 - 0.352	0.352 - 0.366	0.348 - 0.362	0.343 - 0.353
11	Mean ± SE	0.348 ± 0.003	0.358 ± 0.003	0.362 ± 0.003	0.353 ± 0.003

	95% *CI*	0.342 - 0.354	0.351 - 0.364	0.356- 0.368	0.346 - 0.359
rTPJ					
4	Mean ± SE	0.339 ± 0.002	0.349 ± 0.003	0.347 ± 0.003	0.342 ± 0.003
	95% *CI*	0.334 - 0.344	0.344 - 0.354	0.340 - 0.354	0.336 - 0.349
13	Mean ± SE	0.336 ± 0.003	0.350 ± 0.003	0.346 ± 0.003	0.339 ± 0.003
	95% *CI*	0.330 - 0.342	0.345 - 0.356	0.340 - 0.352	0.333 - 0.344

c, The Role effect under no-bonding control (*n* = 43 sessions) and in-group bonding (*n* = 43 sessions) conditions, respectively

Channel	Effect	*t*	*p*	*Cohen's d*
rDLPFC				
8	Control (defender vs. attacker)	3.106	0.003**	0.474
	Bonding (defender vs. attacker)	-1.586	0.120	-0.242
11	Control (defender vs. attacker)	2.060	0.046*	0.314
	Bonding (defender vs. attacker)	-2.160	0.037*	-0.329
rTPJ				
4	Control (defender vs. attacker)	2.622	0.012*	0.400
	Bonding (defender vs. attacker)	-1.143	0.259	-0.174
13	Control (defender vs. attacker)	3.141	0.003**	0.479
	Bonding (defender vs. attacker)	-1.657	0.105	-0.253

d, The Bonding effect for attacker (*n* = 86 3-person groups) and defender (*n* = 86 3-person groups), respectively

Channel	Effect	*t*	*p*	*Cohen's d*
rDLPFC				
8	Attacker (bonding vs. control)	1.983	0.051	0.428
	Defender (bonding vs. control)	-2.529	0.013*	-0.545

11	Attacker (bonding vs. control)	3.448	8.86×10^{-4}***	0.744
	Defender (bonding vs. control)	-1.100	0.274	-0.237
rTPJ				
4	Attacker (bonding vs. control)	1.866	0.066	0.402
	Defender (bonding vs. control)	-1.737	0.086	-0.375
13	Attacker (bonding vs. control)	2.212	0.030*	0.477
	Defender (bonding vs. control)	-3.112	0.003**	-0.671

Note: **a,** Mixed-model ANOVAs, n = 86 three-versus-three-person intergroup contest sessions, FDR-corrected p: p-value corrected for the interaction effect of 14 channels. Effects and p-values in bold indicate effects survived FDR correction. **c,** Two-tailed paired-samples *t-tests*, 43 three-person attacker groups and 43 three-person defender groups; **d,** Two-tailed independent samples *t-tests*, 43 three-person attacker (defender) groups under in-group bonding and 43 three-person attacker (defender) groups under no-bonding control. * $p < 0.05$, ** $p < 0.01$, *** $p < 0.001$.

Supplementary Table 6 | The Bonding × Role interaction on within-group neural synchronization when including within-group decision similarity in the analysis (*n* = 86 intergroup contest sessions).

Channel	*F*	*p*	*η2*	FDR-corrected *p*
rDLPFC				
2	0.027	0.869	3.32×10^{-4}	0.869
5	0.439	0.510	0.005	0.785
6	0.043	0.836	0.001	0.869
8	11.165	1.26×10^{-3}**	0.120	**9.52×10^{-3}****
11	8.769	0.004**	0.097	**0.019***
12	0.174	0.678	0.002	0.863
14	4.159	0.045*	0.048	0.110
rTPJ				
1	0.340	0.561	0.004	0.785
3	4.080	0.047*	0.047	0.110
4	8.094	0.006**	0.090	**0.021***
7	3.260	0.075	0.038	0.150
9	2.239	0.138	0.027	0.242
10	0.077	0.781	0.001	0.869
13	11.006	1.36×10^{-3}**	0.118	**9.52×10^{-3}****

Note: Within-group decision similarity was calculated as the contribution difference of each pair of the 3-person group for each round [i.e., ($|x_1 - x_2| + |x_2 - x_3| + |x_1 - x_3|$) for attacker group; ($|y_1 - y_2| + |y_2 - y_3| + |y_1 - y_3|$) for defender group]. Mixed model ANCOVAs with within-group decision similarity as a covariate, $n = 86$ three-versus-three-person intergroup contest sessions; * $p < 0.05$, ** $p < 0.01$; FDR-corrected *p*: *p*-value corrected for the interaction effect of 14 channels. Channels and *p*-values in bold indicate effects survived FDR correction.

Supplementary Table 7 | The correlation between within-group neural synchronization and group contribution.

Role	Channel	*r*	*p*	FDR-corrected *p*
Attacker (n = 86)	**8**	0.375	3.70×10^{-4}***	**0.002****
	11	0.188	0.083	0.166
	4	-0.010	0.930	0.930
	13	0.155	0.153	0.204
Defender (n = 86)	8	-0.226	0.036*	0.062
	11	-0.242	0.025*	0.062
	4	-0.216	0.046*	0.062
	13	-0.183	0.091	0.091

Note: Pearson's correlation coefficient analysis for 86 three-person attacker groups and 86 three-person defender groups, respectively. * $p < 0.05$, ** $p < 0.01$, *** $p < 0.001$; FDR-corrected *p*: *p*-value corrected for the prediction strength of the 4 channels, respectively for attacker and defender groups. Channel and *p*-values in bold indicate effects survived FDR correction.

Supplementary Table 8 | Full statistical reports for the group-averaged functional connectivity (GFC) of rDLPFC-rTPJ (*n* = 86 intergroup contest sessions).

a, Descriptive statistics for grand mean GFC of rDLPFC-rTPJ

Indices	No-bonding control (*n* = 43)		In-group bonding (*n* = 43)	
	Attacker	Defender	Attacker	Defender
Mean ± SE	0.531 ± 0.007	0.548 ± 0.007	0.568 ± 0.007	0.558 ± 0.008
95% *CI*	0.518 - 0.545	0.533 - 0.563	0.553 - 0.582	0.542 - 0.575

b, Result of Bonding × Role mixed-model ANOVA on the grand mean GFC (*n* = 86 sessions)

Effect	*F*	*p*	η^2
Bonding	9.035	0.003**	0.097
Role	0.273	0.603	0.003
Bonding × Role	3.349	0.071	0.038

c, The Bonding effect on the channel-pair-wise GFC of rDLPFC-rTPJ (*n* = 86 sessions)

Channel pairs (rDLPFC-rTPJ)	*F*	*p*	η^2	FDR-corrected *p*
CH2-CH1	0.111	0.740	0.001	0.756
CH2-CH3	0.329	0.568	0.004	0.605
CH2-CH4	2.629	0.109	0.030	0.161
CH2-CH7	6.405	0.013*	0.071	**0.043***
CH2-CH9	6.122	0.015*	0.068	**0.044***
CH2-CH10	9.643	0.003**	0.103	**0.017***
CH2-CH13	5.203	0.025*	0.058	0.058
CH5-CH1	1.678	0.199	0.020	0.270
CH5-CH3	3.591	0.062	0.041	0.097
CH5-CH4	3.689	0.058	0.042	0.095
CH5-CH7	10.285	0.002**	0.109	**0.017***
CH5-CH9	11.315	1.16×10^{-3}**	0.119	**0.017***
CH5-CH10	4.367	0.040*	0.049	0.078
CH5-CH13	9.525	0.003**	0.102	**0.017***
CH6-CH1	0.015	0.902	1.83×10^{-4}	0.902

CH6-CH3	0.707	0.403	0.008	0.439
CH6-CH4	3.228	0.076	0.037	0.116
CH6-CH7	7.125	0.009**	0.078	**0.032***
CH6-CH9	8.365	0.005**	0.091	**0.022***
CH6-CH10	6.281	0.014*	0.070	**0.043***
CH6-CH13	8.689	0.004**	0.094	**0.020***
CH8-CH1	0.145	0.704	0.002	0.734
CH8-CH3	1.618	0.207	0.019	0.270
CH8-CH4	1.200	0.276	0.014	0.323
CH8-CH7	4.111	0.046*	0.047	0.086
CH8-CH9	9.306	0.003**	0.100	**0.017***
CH8-CH10	2.426	0.123	0.028	0.177
CH8-CH13	5.409	0.022*	0.060	0.058
CH11-CH1	0.764	0.385	0.009	0.428
CH11-CH3	3.745	0.056	0.043	0.095
CH11-CH4	1.341	0.250	0.016	0.303
CH11-CH7	5.194	0.025*	0.058	0.058
CH11-CH9	14.842	2.28×10^{-4}***	0.150	**0.011***
CH11-CH10	3.931	0.051	0.045	0.091
CH11-CH13	9.939	0.002**	0.106	**0.017***
CH12-CH1	1.360	0.247	0.016	0.303
CH12-CH3	1.599	0.210	0.019	0.270
CH12-CH4	1.019	0.316	0.012	0.360
CH12-CH7	5.147	0.026*	0.058	0.058
CH12-CH9	8.146	0.005**	0.088	**0.022***
CH12-CH10	4.952	0.029*	0.056	0.061
CH12-CH13	5.803	0.018*	0.065	**0.050***
CH14-CH1	1.321	0.254	0.015	0.303
CH14-CH3	3.890	0.052	0.044	0.091
CH14-CH4	1.610	0.208	0.019	0.270
CH14-CH7	10.016	0.002**	0.107	**0.017***
CH14-CH9	11.158	1.25×10^{-3}**	0.117	**0.017***
CH14-CH10	4.770	0.032*	0.054	0.065
CH14-CH13	7.300	0.008**	0.080	**0.031***

Note: The grand mean GFC of rDLPFC-rTPJ was indexed by the averaged 49 coherence value of all channel pairings between the right rDLPFC (i.e. 7 channels within rDLPFC) and rTPJ (i.e. 7 channels within rTPJ) within 3-person group[1]; The 49 channel-pair-wise GFC were indexed by the averaged coherence value from each rDLPFC-rTPJ channel pairings within 3-person group. FDR correction in Table **c** was applied for the main effect of Bonding in all 49 channel pairs; Mixed-model ANOVAs, n = 86 three-versus-three-person intergroup contest sessions; Significance value in bold survived FDR correction. * $p < 0.05$, ** $p < 0.01$, *** $p < 0.001$.

References:

1. Zhang, L. et al. Studying hemispheric lateralization during a Stroop task through near-infrared spectroscopy-based connectivity. *J. Biomed. Opt*. **19**, 057012 (2014).

Supplementary Table 9 | Results of Within-group Neural Synchronization after controlling for global mean (*n* = 86 intergroup contest sessions).

a, The Bonding × Role interaction on GNS after controlling for global mean (*n* = 86 sessions)

Channel	*F*	*p*	η^2	FDR- corrected *p*
rDLPFC				
2	0.090	0.764	0.001	0.895
5	1.342	0.250	0.016	0.389
6	0.483	0.489	0.006	0.685
8	9.522	0.003**	0.103	**0.022***
11	9.262	0.003**	0.100	**0.022***
12	0.046	0.831	0.001	0.895
14	4.333	0.040*	0.050	0.081
rTPJ				
1	0.067	0.797	0.001	0.895
3	5.646	0.020*	0.064	0.069
4	5.057	0.027*	0.057	0.076
7	4.577	0.35*	0.052	0.081
9	2.561	0.113	0.030	0.198
10	0.006	0.939	7.12×10^{-5}	0.939
13	6.669	0.012*	0.074	0.054

b, Correlation between within-group neural synchronization and group contributions

Role	Channel	*r*	*p*	FDR-corrected *p*
Attacker	**8**	0.388	2.40×10^{-4}***	**4.80×10^{-4}***
(*n* =86)	**11**	0.222	0.041	**0.041***
Defender	**8**	-0.253	0.020**	**0.040***
(*n* =86)	11	-0.205	0.060	0.060

Note: **a,** Mixed-model ANCOVAs, *n* = 86 three-versus-three-person intergroup contest sessions, with GNS global mean as a covariate. FDR-corrected *p*: *p*-value corrected for the interaction effect of 14 channels. **b,** Pearson's correlation analysis for 86 attacker groups and 86 defender groups, respectively. FDR-corrected p: p-value corrected for 2 channels showing Bonding × Role interaction. *p*-values in bold indicate effects survived FDR correction; * $p < 0.05$; ** $p < 0.01$; *** $p < 0.001$;

Supplementary Table 10 | Gender effect on the within-group neural synchronization (a), within-group averaged neural activity (b), and group-level functional connectivity (c).

a, Gender effect on the within-group neural synchronization (*n* = 86 integroup contest sessions)

Channel	Effect	*F*	*p*	η^2	FDR-corrected *p*
rDLPFC					
2	Gender	0.003	0.953	4.19×10^{-5}	0.953
	Gender × Bonding	0.782	0.379	0.009	0.666
	Gender × Role	0.043	0.837	0.001	0.905
	Gender × Bonding × Role	1.222	0.272	0.015	0.762
5	Gender	3.513	0.064	0.041	0.138
	Gender × Bonding	1.72×10^{-6}	0.999	2.10×10^{-8}	0.999
	Gender × Role	0.014	0.905	1.75×10^{-4}	0.905
	Gender × Bonding × Role	3.376	0.070	0.040	0.490
6	**Gender**	11.085	1.31×10^{-3}**	0.119	**0.018***
	Gender × Bonding	0.001	0.980	8.04×10^{-6}	0.999
	Gender × Role	0.125	0.724	0.002	0.905
	Gender × Bonding × Role	0.062	0.804	0.001	0.939
8	**Gender**	8.689	0.004**	0.096	**0.029***
	Gender × Bonding	0.287	0.593	0.003	0.692
	Gender × Role	0.017	0.896	2.10×10^{-4}	0.905
	Gender × Bonding × Role	0.447	0.506	0.005	0.939
11	Gender	5.385	0.023*	0.062	0.080
	Gender × Bonding	1.165	0.284	0.014	0.666
	Gender × Role	0.028	0.868	3.41×10^{-4}	0.905
	Gender × Bonding × Role	4.601	0.035*	0.053	0.490

12	Gender	1.633	0.205	0.020	0.341
	Gender × Bonding	1.723	0.193	0.021	0.666
	Gender × Role	2.405	0.125	0.028	0.546
	Gender × Bonding × Role	0.049	0.825	0.001	0.939
14	Gender	0.241	0.625	0.003	0.729
	Gender × Bonding	0.824	0.367	0.010	0.666
	Gender × Role	2.054	0.156	0.024	0.546
	Gender × Bonding × Role	1.376	0.244	0.016	0.762
rTPJ					
1	Gender	0.929	0.338	0.011	0.473
	Gender × Bonding	0.489	0.487	0.006	0.666
	Gender × Role	4.174	0.044*	0.048	0.546
	Gender × Bonding × Role	0.117	0.734	0.001	0.939
3	Gender	0.547	0.462	0.007	0.587
	Gender × Bonding	1.607	0.209	0.019	0.666
	Gender × Role	0.595	0.443	0.007	0.905
	Gender × Bonding × Role	0.129	0.720	0.002	0.939
4	Gender	3.390	0.069	0.040	0.138
	Gender × Bonding	0.603	0.440	0.007	0.666
	Gender × Role	3.058	0.084	0.036	0.546
	Gender × Bonding × Role	0.041	0.839	0.001	0.939
7	Gender	0.099	0.754	0.001	0.812
	Gender × Bonding	0.787	0.378	0.010	0.666
	Gender × Role	0.224	0.638	0.003	0.905
	Gender × Bonding × Role	0.026	0.872	3.17×10^{-4}	0.939

9	Gender	1.534	0.219	0.018	0.341
	Gender × Bonding	0.411	0.523	0.005	0.666
	Gender × Role	0.039	0.843	$4.81{\times}10^{-4}$	0.905
	Gender × Bonding × Role	0.001	0.970	$1.76{\times}10^{-5}$	0.970
10	Gender	4.732	0.032*	0.055	0.091
	Gender × Bonding	1.568	0.214	0.019	0.666
	Gender × Role	0.029	0.865	$3.52{\times}10^{-4}$	0.905
	Gender × Bonding × Role	0.656	0.420	0.008	0.939
13	**Gender**	7.142	0.009**	0.080	**0.042***
	Gender × Bonding	0.442	0.508	0.005	0.666
	Gender × Role	1.685	0.198	0.020	0.554
	Gender × Bonding × Role	1.677	0.199	0.020	0.762

b, The Gender effect on the within-group neural activity (*n* = 86 sessions)

Effect	*F*	*p*	η^2
Gender	2.815	0.097	0.033

c, The Gender effect on the within-group functional connectivity of rDLPFC-rTPJ (*n* = 86 sessions).

Channel pairs (rDLPFC-rTPJ)	F	*p*	η^2	FDR-corrected *p*
Grand mean	1.169	0.283	0.014	-
CH2-CH7	0.518	0.474	0.006	0.790
CH2-CH9	0.177	0.675	0.002	0.797
CH2-CH10	2.063	0.155	0.025	0.612
CH5-CH7	8.835	0.004**	0.097	0.070

CH5-CH9	3.114	0.081	0.037	0.488
CH5-CH13	0.405	0.526	0.005	0.790
CH6-CH7	3.336	0.071	0.039	0.488
CH6-CH9	1.918	0.170	0.023	0.612
CH6-CH10	0.818	0.368	0.010	0.790
CH6-CH13	0.075	0.785	0.001	0.831
CH8-CH9	1.163	0.284	0.014	0.730
CH11-CH9	0.238	0.627	0.003	0.797
CH11-CH13	0.020	0.889	2.41×10^{-4}	0.889
CH12-CH9	0.268	0.607	0.003	0.797
CH12-CH13	1.401	0.240	0.017	0.720
CH14-CH7	0.441	0.509	0.005	0.790
CH14-CH9	0.702	0.405	0.008	0.790
CH14-CH13	0.141	0.708	0.002	0.797

Note: **a-c,** Mixed-model ANOVAs, n = 86 three-versus-three-person intergroup contest sessions; **a,** FDR-corrected *p*: *p*-value corrected for the main effect of Gender and Gender-related interaction effects on GNS in 14 channels. Effects and *p*-values in bold indicate effects survived FDR correction; **c.** FDR-corrected *p*: *p*-value corrected for the main effect of Gender on rDLPFC-rTPJ connectivity in at 18 channel pairs where we showed significant Bonding effect on rDLPFC-rTPJ connectivity; * $p < 0.05$, ** $p < 0.01$.

Supplementary Table 11 | Full statistical reports for the group-level functional connectivity (GFC) of rDLPFC-rTPJ (*n* = 86 intergroup contest sessions).

Channel pairs (rDLPFC-rTPJ)	*F*	*p*	η^2	FDR-corrected *p*
CH2-CH1	0.405	0.526	0.005	0.586
CH2-CH3	0.043	0.837	0.001	0.873
CH2-CH4	0.028	0.867	3.37×10^{-4}	0.882
CH2-CH7	0.022	0.882	2.62×10^{-4}	0.882
CH2-CH9	0.198	0.657	0.002	0.716
CH2-CH10	2.003	0.161	0.023	0.239
CH2-CH13	1.102	0.297	0.013	0.364
CH5-CH1	0.628	0.430	0.007	0.490
CH5-CH3	0.731	0.395	0.009	0.461
CH5-CH4	6.367	0.014*	0.070	0.073
CH5-CH7	9.126	0.003**	0.098	**0.048***
CH5-CH9	3.853	0.053	0.044	0.106
CH5-CH10	7.699	0.007 **	0.084	0.067
CH5-CH13	3.204	0.077	0.037	0.135
CH6-CH1	2.553	0.114	0.030	0.180
CH6-CH3	1.768	0.187	0.021	0.268
CH6-CH4	1.665	0.201	0.019	0.268
CH6-CH7	3.743	0.056	0.043	0.106
CH6-CH9	6.270	0.014*	0.069	0.073
CH6-CH10	1.695	0.196	0.020	0.269
CH6-CH13	3.519	0.064	0.040	0.116
CH8-CH1	2.796	0.098	0.032	0.161
CH8-CH3	4.030	0.048*	0.046	0.106
CH8-CH4	4.643	0.034*	0.052	0.106
CH8-CH7	4.508	0.037*	0.051	0.106
CH8-CH9	6.959	9.93×10^{-3}**	0.077	0.073
CH8-CH10	1.648	0.203	0.019	0.268
CH8-CH13	4.129	0.045*	0.047	0.106
CH11-CH1	0.934	0.337	0.011	0.402
CH11-CH3	3.797	0.055	0.043	0.106

CH11-CH4	4.123	0.045*	0.047	0.106
CH11-CH7	5.453	0.022*	0.061	0.090
CH11-CH9	8.952	0.004**	0.096	**0.048***
CH11-CH10	1.325	0.253	0.016	0.326
CH11-CH13	6.852	0.011*	0.075	0.073
CH12-CH1	4.039	0.048*	0.046	0.106
CH12-CH3	2.145	0.147	0.025	0.225
CH12-CH4	3.783	0.055	0.043	0.106
CH12-CH7	3.030	0.085	0.035	0.144
CH12-CH9	8.783	0.004**	0.095	**0.048***
CH12-CH10	0.098	0.755	0.001	0.804
CH12-CH13	3.936	0.051	0.045	0.106
CH14-CH1	3.764	0.056	0.043	0.106
CH14-CH3	5.734	0.019*	0.064	0.084
CH14-CH4	6.181	0.015*	0.069	0.073
CH14-CH7	4.341	0.040*	0.049	0.106
CH14-CH9	11.320	1.16×10^{-3}**	0.119	**0.048***
CH14-CH10	1.167	0.283	0.014	0.356
CH14-CH13	3.786	0.055	0.043	0.106

Note: We first averaged the denoised Oxy-Hb neural activity in each channel across 3 participants of each real or pseudo group. We then performed coherence analyses between each of the 7 channels in the rDLPFC with each of the 7 channels in the rTPJ (i.e., 49 channel pairs) to index channel-pairwise group-level functional connectivity (GFC) of rDLPFC–rTPJ and submitted the channel-pairwise GFC to Role-by-Bonding ANOVAs. Mixed-model ANOVAs, $n = 86$ three-versus-three-person intergroup contest sessions; * $p < 0.05$, ** $p < 0.01$; FDR-corrected *p*: *p*-value corrected for the main effect of Bonding in all 49 channel pairs. Channel pairs and *p*-values in bold indicate effects survived FDR correction.